ORIGINAL PAPER

Removal of siloxanes from biogas using acetylated silica gel as adsorbent

Yu-Heng Liu[1,2] · Ze-You Meng[1] · Ji-Ye Wang[1] · Yan-Fei Dong[1] · Zi-Chuan Ma[1]

Abstract

Biogas can be used as an alternative energy source for producing heat and electricity; however, volatile methylsiloxanes (VOSiC) present in biogas can severely damage heat exchangers, turbines and gas engines. Consequently, efficient removal of VOSiC from biogas that is used as a biofuel is required. In this work, acetylated silica gel (Ac@SG) was synthesized, via treatment of microporous silica gel (SG) with acetic anhydride as an adsorbent, for removal of VOSiC from biogas, and characterized with XRD, SEM–EDS, N_2-BET and FT-IR. This Ac@SG adsorbent exhibited a meso-/microporous structure and hydrophobic surface, indicating it was a more efficient adsorbent for removing hexamethyldisiloxane (L2) and octamethylcyclotetrasiloxane (D4) from biogas samples than conventional SG. It was found that the adsorption capacities of Ac@SG reached 304 mg L2/g for hexamethyldisiloxane and 916 mg D4/g for octamethylcyclotetrasiloxane at lower temperatures in the experimental range, and water had no significant effect on its absorption efficiency. The used Ac@SG could be easily regenerated by heating it at 110 °C, and the adsorption capacity of recycled Ac@SG for hexamethyldisiloxane and octamethylcyclotetrasiloxane was kept constant in four recycle adsorption experiments.

Keywords Siloxanes · Biogas · Acetylated silica gel · Adsorption · Removal of the siloxanes

1 Introduction

Climate change and the end of the 'cheap oil' era have prompted investigations into the technical and financial resources required to replace fossil fuels with renewable energy sources (de Arespacochaga et al. 2014), such as the waste materials from industrial and domestic sources available as potential energy sources. Biogas is produced by the anaerobic digestion of organic matter in landfill and sewage plants. Biogas is primarily comprised of methane CH_4 (50%–70%) and carbon dioxide CO_2 (30%–50%), as well as trace amounts of other components, such as hydrogen sulfide, halogenated compounds, volatile organic compounds (VOCs) and siloxanes (Kougias and Angelidaki 2018; Devia and Subrenat 2013). Currently, the use of biogas as a renewable energy sources is complicated due to the presence of siloxane contaminants, which are transformed into microcrystalline SiO_2 at high temperatures, whose abrasiveness and thermoelectric insulating properties can severely damage heat exchangers, turbines and gas engines (Turkin et al. 2014; Lee and Rittmann 2016; Allen et al. 1997). Consequently, it is necessary to reduce the amount of siloxanes in biogas below a threshold level (e.g., 10 mg siloxane/m^3 of methane) if it is to be used as a biofuel for energy applications (Devia and Subrenat 2013; Lee and Rittmann 2016; Dewil et al. 2006). Several methods are used in industry to remove siloxanes from biogas, including adsorption by porous materials (Sigot et al. 2015; Jiang et al. 2016; Jafari et al. 2016) and oils (Devia and Subrenat 2013); however, their performance is often unsatisfactory, because they employ expensive or non-recyclable materials, involve long treatment time and high energy consumption,

✉ Zi-Chuan Ma
  mazc@hebtu.edu.cn

[1] College of Chemistry and Material Science, Hebei Normal University, Shijiazhuang 050024, Hebei, China

[2] College of Pharmaceutical Sciences, Hebei Medical University, Shijiazhuang 050017, Hebei, China

and only afford low saturation adsorption levels (Kajolinna et al. 2015; Ajhar et al. 2010). Therefore, it is necessary to find a more effective method that employs recyclable materials to remove siloxanes from biogas so that it can be used as a renewable fuel. Adsorption techniques are one of the simplest techniques used for gas purification (Ajhar et al. 2010), with silica gel (SG) often used to adsorb organic compounds, such as alkanes, toluene, 2,4,6-trinitrotoluene and herbicides (Machin and Golding 1987; Sui et al. 2017a, b; An et al. 2009; Koner et al. 2013). In this work, acetylated silica gel (Ac@SG) was studied as an adsorbent for removal of siloxanes from biogas, and it was found to exhibit better adsorption properties for hexamethyldisiloxane and octamethylcyclotetrasiloxane than pristine SG.

2 Materials and methods

2.1 Chemicals and materials

All the chemicals and reagents used in this study were of analytical grade. Microporous silica gel (SG) was obtained from Liang Chen Silicon Material Co. Limited, Anhui Province, China. Hexamethyldisiloxane (L2, 99%) and octamethylcyclotetrasiloxane (D4, 99%) used as representative siloxanes for adsorption experiments were obtained from Tokyo Chemical Industry Co. Limited, Tokyo, Japan. Acetic anhydride was purchased from Rionlon Bohua Pharmaceutical & Chemical Co. Limited, Tianjin, China.

2.2 Preparation of acetylated silica gel

2.2.1 Activation of silica gel

Silica gel (50 g) was refluxed with an excess of HCl (18.5%, v/v) solution for 12 h, then filtered off and washed with deionized water until no detectable chloride ion could be found in the filtrate. The resultant activated silica was then dried at 150 °C for 12 h to remove any adsorbed water from its surface (Ahmed 2014; Uruş et al. 2013; Çimen et al. 2015).

2.2.2 Modification of silica gel with acetic anhydride

Acetic anhydride (7.4 mL) was added to activated silica gel (3.0 g) at room temperature, and the mixture was then stirred at 90 °C for 10 h. The mixture was then separated by filtration and the solid soaked in deionized water for 30 min, before being washed with deionized water until the washings were neutral. The resultant solid was then dried in an oven at 110 °C for 12 h to afford the desired acetylated silica gel (Ac@SG) (Damja and Eaborn 1985; Eaborn et al. 1988).

2.3 Characterization methods

The surface morphology of adsorbents was studied using a Hitachi S-4800 scanning electron microscope (SEM). Elemental compositions were determined on the SEM, which was equipped with an INCA 350 energy-dispersive spectrometer (EDS) operating at 133 eV resolution at 5.9 KeV. Nitrogen adsorption/desorption isotherms were measured at −196 °C using an automatic surface area and pore analyzer (Kubo×1000, Beijing Builder Co., China), with all samples being degassed at 200 °C for 3 h before analysis. Specific surface areas (S_{BET}) and micropore volumes (V_{micro}) were calculated using the Brunauer–Emmett–Teller (BET) equation and Dubinin–Radushkevich (DR) method, respectively. The total pore volume (V_t) was estimated from the liquid volume of N_2 adsorbed at a relative pressure of 0.99. Pore size distribution curves were obtained using the Barrett–Joyner–Halenda (BJH) method. X-ray diffraction (XRD) analysis was carried out using a Bruker D8 ADVANCE X-ray diffractometer. Fourier transform infrared (FT-IR) spectra were recorded over a range of 4000–400 cm^{-1} with KBr pellets using a Bruker Tensor 27 spectrometer (Bruker Optics Co., Germany).

2.4 Siloxane adsorption setup and procedure

Concentrations of siloxanes (L2 and D4) were measured using gas chromatography employing a hydrogen flame ionization detector (GC/FID). The adsorption measurement apparatus used for evaluation of samples is shown in Fig. 1. Nitrogen flow containing a defined percentage of L2 or D4 was passed through a quartz tube (8 mm) containing an appropriate bed height of adsorbent. The volume ratio of a model gas to N_2 was obtained by mixing two nitrogen flows from a cylinder (99.9%). The first flow, F1, was bubbled through a bottle filled with liquid siloxane (L2 or D4), with the resultant stream enriched in vaporized siloxane, then mixed and diluted by the F2 nitrogen stream. The F1 and F2 flows were controlled using two mass flow controllers, MFC1 (0–100 mL/min) and MFC2 (0–100 mL/min), which were calibrated separately using the L2-in-N_2 and D4-in-N_2 feed gas. This enabled a stable concentration of siloxane gas to be obtained using this mixing setup, with the concentration of L2 and D4 in the model gas adjusted to 83.8 and 7.9 mg/L, respectively.

Preliminary measurements were taken by passing the input stream through an adsorbent before every test in order to adjust the concentration level of the model gas. The mixed stream was then sent to the adsorption bed, with the exit gas then sent to the GC/FID for analysis. The adsorption column was operated until the siloxane outlet concentration matched the inlet concentration (i.e., bed exhaustion), with

Fig. 1 Schematic of the siloxane adsorption measurement apparatus
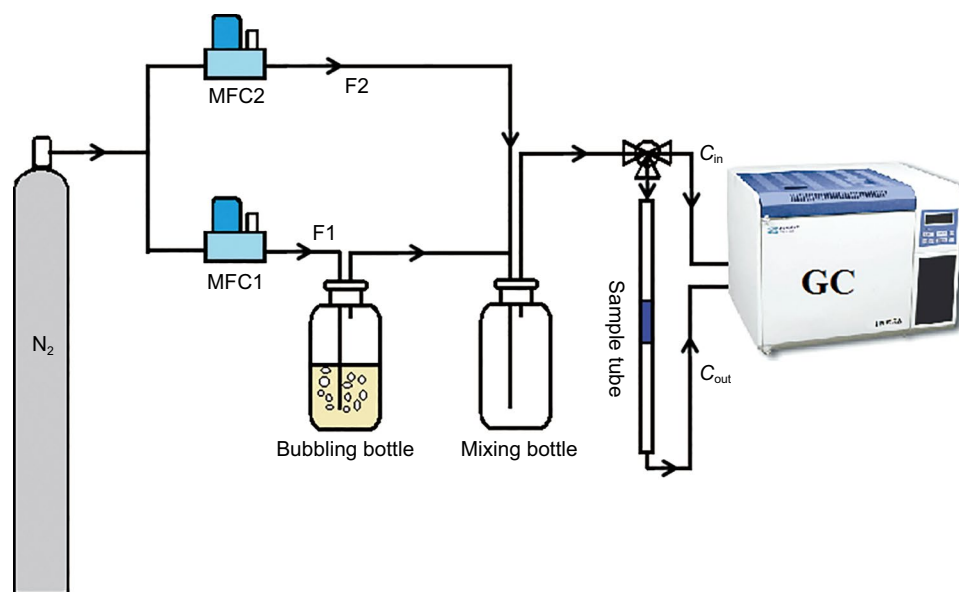
breakthrough curves obtained by plotting $C_{out,t}/C_{in}$ versus time. Adsorbent performance was estimated using three indicators: (1) the breakthrough time t_B (min), which is defined as the time taken for the ratio $C_{out,t}/C_{in}$ to be equal to 0.05; (2) the siloxane (L2 and/or D4) adsorption capacity at t_B (Q_B, mg/g); and (3) the siloxane (L2 and/or D4) adsorption capacity at saturation (Q_m, mg/g). This enabled Q_B and Q_m values for a semi-batch dynamic adsorption experiment, carried out using a continuous flow of gas and a fixed quantity of adsorbent, to be calculated using Eq. (1).

$$Q_t = \frac{V_q C_{in}}{m} \int_0^t (1 - \frac{C_{out,t}}{C_{in}}) \mathrm{d}t \tag{1}$$

where V_q is the gas flow rate (L/min); m is the mass of the adsorbent (g); C_{in} and $C_{out,t}$ are the inlet and outlet siloxane concentration in the gas flow (mg/L), respectively; t is the adsorption time, with integrated adsorption capacities Q_t calculated for every t value. Q_B was obtained when t is equal t_B, with Q_m calculated over the period from $t=0$ to the point of saturation ($C_{out,t}/C_{in} \approx 1$).

3 Results and discussion

3.1 Characterization of the physical properties of SG and Ac@SG

The XRD patterns of SG and Ac@SG are shown in Fig. 2, with the Ac@SG sample showing identical diffraction
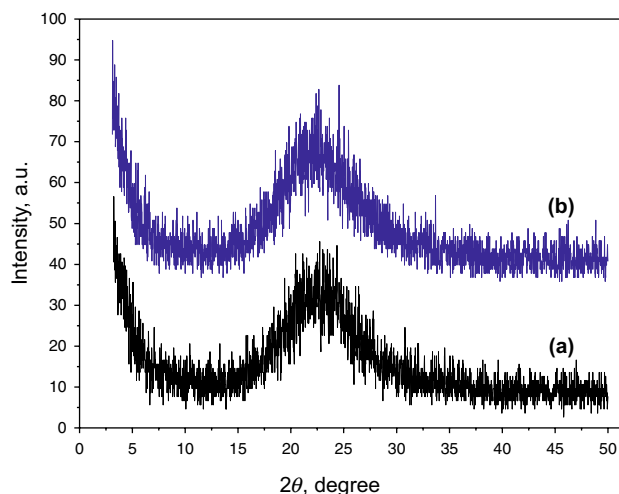

Fig. 2 XRD patterns of SG (**a**) and Ac@SG (**b**)

patterns to those for SG, with no additional peaks for any other crystalline substances being present. This implies that acetylation occurs on the surface of the silica gel, with no modification of its skeleton having occurred. Comparison of the elemental composition of SG and Ac@SG using EDS confirmed the presence of carbon originating from the acetyl groups (Fig. 3). Comparison of the FT-IR spectra of the Ac@SG sample (Fig. 4b) with the FT-IR spectra of SG (Fig. 4a) revealed the presence of three additional well-defined bands at 2996, 1706 and 1379 cm^{-1}. These absorbances were attributed to the C–H stretching
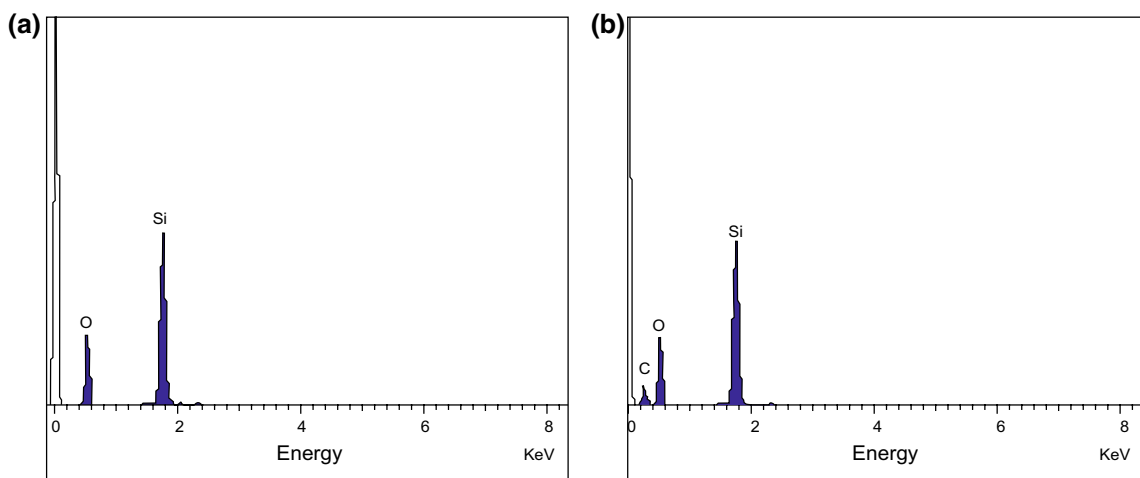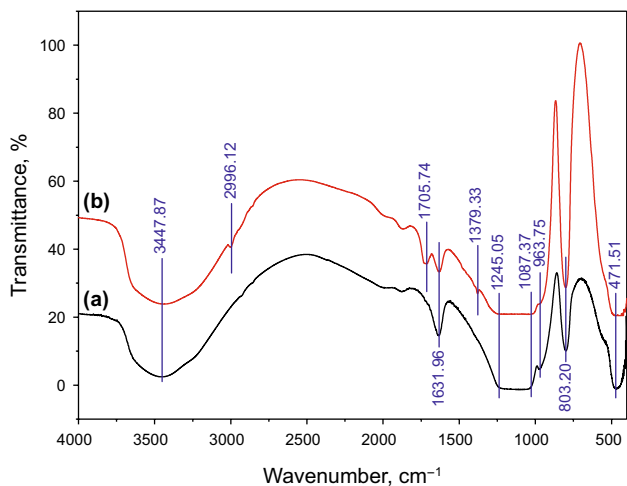
Fig. 3 EDS spectrum of SG (**a**) and Ac@SG (**b**)

Fig. 4 FT-IR spectra of SG (**a**) and Ac@SG (**b**)

vibration of the CH_3 group, the C=O stretching vibration and the C–H bending vibrations of CH_3 groups of its acetyl groups (Pei and Ponec 1996; Mobaraki and Hemmateenejad 2011). A strong absorption at 3447 cm^{-1} was assigned to the O–H stretching vibration and a peak at 1632 cm^{-1} assigned to the O–H bending vibrations of surface silanol groups and adsorbed water molecules. A broadband at 1087–1245 cm^{-1} was attributed to the antisymmetric stretching vibration of Si–O–Si groups, with bands at 964, 803 and 472 cm^{-1} assigned to the stretching and bending vibrations of Si–O groups (Sui et al. 2016; Mota et al. 2017).

The adsorption properties of SG and Ac@SG were analyzed using a N_2-BET method. N_2 adsorption–desorption isotherms indicating that both samples exhibited a typical type IV isotherm (see Fig. 5 and Table 1). Hysteresis loop results and pore size distribution curves reveal that SG and Ac@SG
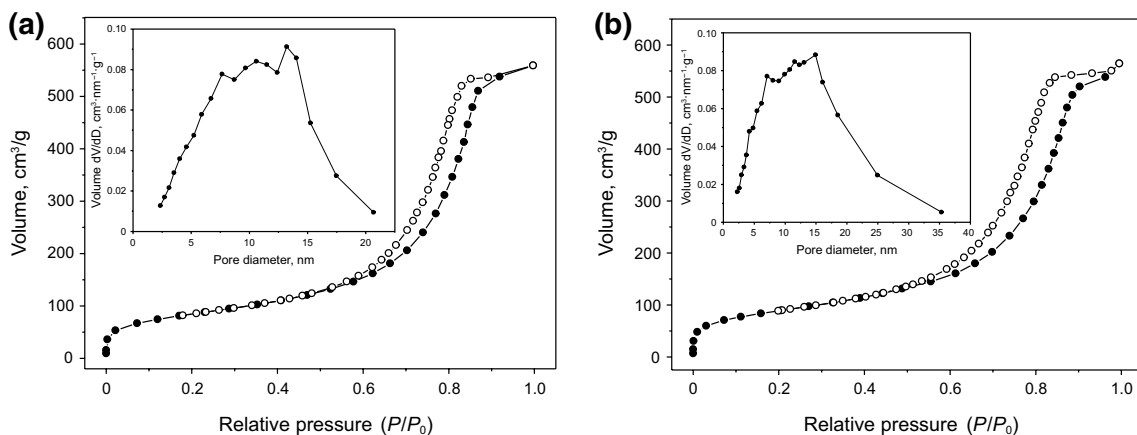

Fig. 5 N_2 adsorption–desorption isotherms and pore size distributions (inset) of SG (**a**) and Ac@SG (**b**)

Table 1 Texture parameters of SG and Ac@SG

Sample	Specific surface area, m^2/g		Pore volume, cm^3/g		Average pore diameter, nm
	S_{BET}	$S_{micro,DR}$	$V_{micro, DR}$	V_{total}	d_{BJH}
SG	286	259	0.13	0.74	10.1
Ac@SG	369	356	0.16	0.86	13.8

were meso-/microporous materials, with average pore diameters of 10.1 and 13.8 nm, respectively. The specific surface area, micropore specific surface area, total pore volume and micropore volume of Ac@SG were all significantly greater than for SG, implying that the texture parameters of Ac@SG should be more favored for siloxane adsorption.

3.2 Comparison of the adsorption properties of SG and Ac@SG

Dynamic adsorption tests revealed that the breakthrough time (t_B) for Ac@SG was significantly greater than for SG for L2 and D4 adsorption (see Fig. 6 and Table 2), with Q_B values for Ac@SG of 282 mg L2/g and 851 mg D4/g, and corresponding to Q_m values for SG of 304 mg L2/g and 916 mg D4/g, respectively. These results imply that adsorption of nonpolar siloxanes by Ac@SG is favored by the more hydrophobic acetyl groups present on its surface, which can be certified by a semiquantitative comparison in Washburn's method (shown in Fig.

S1 in supplementary material). In addition, the reason of different adsorption results between D4 and L2 might be related to the nonpolar proportion and molecular weight of D4, which are both larger than that L2.

3.3 Optimization of the synthesis of Ac@SG

A series of optimization reactions revealed that the best conditions for preparing Ac@SG adsorbent with an optimal capacity for adsorbing siloxanes involved use of a 3:8 ratio of SG to acetic anhydride at 90 °C for 10 h (see Table 3).

3.4 Influence of inlet concentration (C_{in}) on adsorption of Ac@SG

The concentration of siloxanes present in different sources of landfill gases or biogas is variable; therefore, it was necessary to determine the breakthrough times (t_B) of the Ac@SG adsorbent for different concentrations of siloxane. Various concentrations of simulated gas (Table 4, L2 or D4) were produced by regulating the gas flow rates of two mass flow controllers (MFC1 and MFC2), with t_B increasing for decreased inlet concentrations. The breakthrough times for Ac@SG were determined from curves correlating C_{in} (L2 or D4) to t_B (Fig. 7) that enabled the influence of initial siloxane concentration on adsorption performance to be determined. The fitted data for L2 and D4 are shown in Fig. 7a, b, which exhibit correlation coefficients (R^2) of 0.9993 and 0.9992, respectively. Therefore, breakthrough times for these
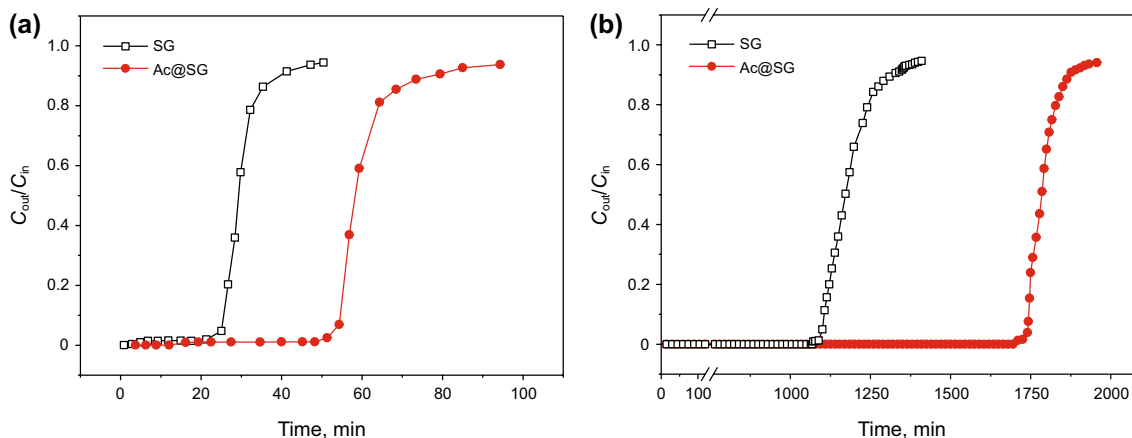
Fig. 6 Breakthrough curves of L2 (**a**) and D4 (**b**)

Table 2 Adsorption comparison of SG and Ac@SG for L2 and D4

Adsorbent	t_B, min		Q_B, mg/g		Q_m, mg/g	
	L2	D4	L2	D4	L2	D4
SG	25.0	1100	105	538	136	602
Ac@SG	54.3	1740	282	851	304	916

Mass of adsorbents = 0.8 g, C_{in}: L2 = 83.8 mg/L, D4 = 7.9 mg/L, Gas flow rate = 50 mL/min

Table 3 Preparation conditions of Ac@SG and the adsorption indicators for L2

Entry	Temperature, °C	Time, h	Ratio[a]	t_B, min	Q_B, mg/g	Q_m, mg/g
1	Room temperature	6	3:7	34.3	178	196
2	50	6	3:7	36.5	189	208
3	70	6	3:7	38.8	201	220
4	90	6	3:7	41.8	217	236
5	110	6	3:7	41.8	2177	236
6	90	5	3:7	39.1	203	223
7	90	7	3:7	43.9	228	248
8	90	8	3:7	45.8	238	258
9	90	9	3:7	48.2	250	271
10	90	10	3:7	51.1	265	286
11	90	12	3:7	51.1	265	286
12	90	10	3:5	38.9	202	223
13	90	10	3:6	45.9	238	260
14	90	10	3:8	54.3	282	304
15	90	10	3:9	54.3	282	304

$M_{Ac@SG} = 0.8$ g, $C_{in, L2} = 83.8$ mg/L, gas flow rate = 50 mL/min

[a]The mass ratio of silica gel to anhydride

Table 4 Influence of the L2 and D4 inlet concentration

Entry	L2		D4	
	C_{in}, mg/L	t_B, min	C_{in}, mg/L	t_B, min
1	83.8	54.3	7.9	215
2	73.7	61.4	6.3	269
3	63.8	70.6	4.7	358
4	47.4	86.2	4.0	430
5	38.3	99.3	3.2	537
6	31.0	116	–	–
7	23.1	150	–	–
8	17.9	182	–	–

$M_{Ac@SG, L2} = 0.8$ g, $M_{Ac@SG, D4} = 0.1$ g

supports can be predicted for L2 and D4 using Eqs. (2) and (3), thus enabling their results which are used to provide data for their industrial use.

$$t_{B, L2} = 398.0 \times e^{-\frac{C_{in}}{11.3}} + 1.5 \times 10^6 \times e^{-\frac{C_{in}}{2.2 \times 10^6}} - 1.5 \times 10^6 \quad (2)$$

$$t_{B, D4} = 1361.4 \times e^{-0.4 \times C_{in}} + 164.0 \quad (3)$$

3.5 Influence of temperature on adsorption properties of Ac@SG

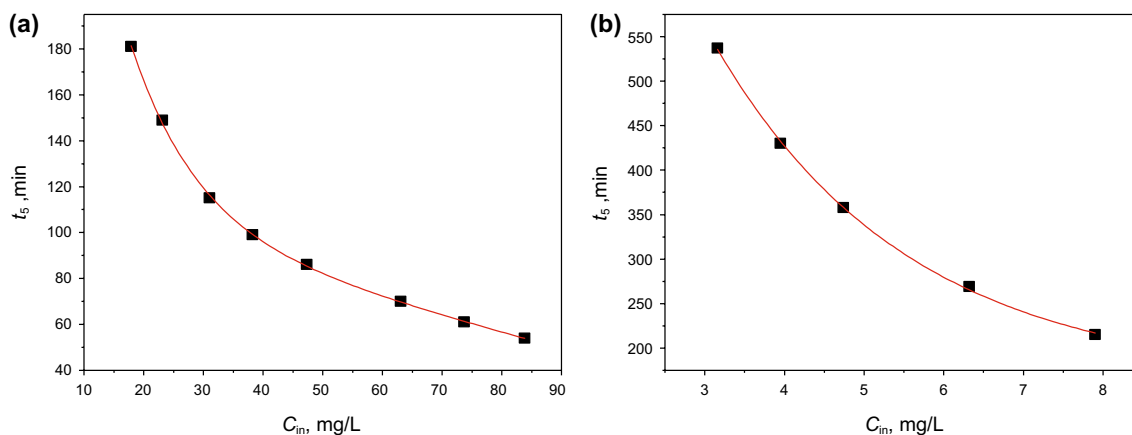The influence of temperature on the adsorption of Ac@SG for L2 and D4 is shown in Table 5, with t_B and Q_B values

Fig. 7 Relationship between breakthrough time (t_B) and the inlet concentrations (C_{in}) of L2 (**a**) and D4 (**b**)

Table 5 Influence of the temperature on the adsorption of L2 and D4

Entry	L2[a]			D4[b]		
	Temperature, °C	t_B, min	Q_B, mg/g	Temperature, °C	t_B, min	Q_B, mg/g
1	0	121	628	20	215	842
2	10	82.1	426	30	134	524
3	25	54.3	282	40	85.9	336
4	45	33.2	172	50	51.7	202
5	60	25.9	134	60	35.5	139

The amount of adsorbent is shown in Table 4

[a]$C_{in, L2} = 83.8$ mg/L; [b]$C_{in, D4} = 7.9$ mg/L

Table 6 Influence of the adsorbent bed height and masses on the adsorption of L2 and D4

Entry[a]	Ac@SG, g	Bed height, mm	t_B, min	Total adsorbed amount, mg	Q_B, mg/g
1	0.2	10.0	13.4	51.1	278
2	0.4	20.0	26.9	104	279
3	0.6	30.0	40.5	159	280
4	0.8	40.0	54.3	214	282
5	0.1	5.0	215	74.1	842
6	0.3	15.0	647	230	843
7	0.5	25.0	1080	391	845
8	0.8	40.0	1741	629	851

$C_{in, L2} = 83.8$ mg/L; $C_{in, D4} = 7.9$ mg/L

[a]The data of entries (1–4) were L2, and others were D4

greater at lower temperatures, which means that the adsorption performance of Ac@SG is better at lower temperatures than that at higher temperatures. These results are in accordance with the results of Sigot et al. (2014), with the exothermic micropore adsorption and hydrophobic effects of the meso-/micro-porous skeletons and acetyl groups of Ac@SG resulting in good adsorption properties at lower temperatures.

3.6 Influence of bed height and mass of Ac@SG adsorbent

Dynamic adsorption tests were performed using different masses of Ac@SG in order to explore the combined influence of bed height and quantity of adsorbent on the efficiency of siloxane removal. As expected, increasing adsorbent bed height resulted in breakthrough times being delayed (Table 6, t_B, entries 1–4 or 5–8), with the total amount of L2 and D4 adsorbed found to be directly proportional to the mass of Ac@SG used. These results indicate that Q_B was not significantly affected by the adsorbent bed height (Ac@SG mass) during the experiment process (see Table 6), with adsorption capacity range of 278–282 mg L2/g Ac@SG and 842–851 mg D4/g Ac@SG, respectively. These adsorption values mean that Ac@SG can absorb siloxanes at significantly lower concentration levels than conventional silica gel adsorbents (Matsui and Imamura 2010; Schweigkofler and Niessner 2001; Oshita et al. 2010).

3.7 Influence of the presence of water on Ac@SG adsorbent

Biogas is usually saturated with water at digester or landfill outlets (Sigot et al. 2014); therefore, the influence of water on the ability of silica gel (a desiccant) to adsorb siloxanes was evaluated. The ability of Ac@SG to remove L2 and D4 from dry and moist gas (RH of 70%) is shown in Fig. 8, with water having no significant effect on the ability of Ac@SG to remove L2 and D4. This phenomenon is likely to be due to the presence of hydrophobic acetyl groups on the surface of Ac@SG which reduced its ability to absorb water. Therefore, Ac@SG has a better affinity for L2 and D4 than water, meaning that Ac@SG can be used as an adsorbent for siloxanes from wet biogas sources.

3.8 Thermal regeneration

The thermal regeneration and reusability of a used Ac@SG sample that had been employed for L2 adsorption were then assessed by desorbing it at 110 °C for 2 h and then reusing it as an adsorbent in consecutive siloxane adsorption experiments, under the same conditions. Adsorption results revealed that breakthrough times remained between 48 min to 54 min, even after the same Ac@SG sample was reused for five cycles of siloxane adsorption (see Fig. 9).
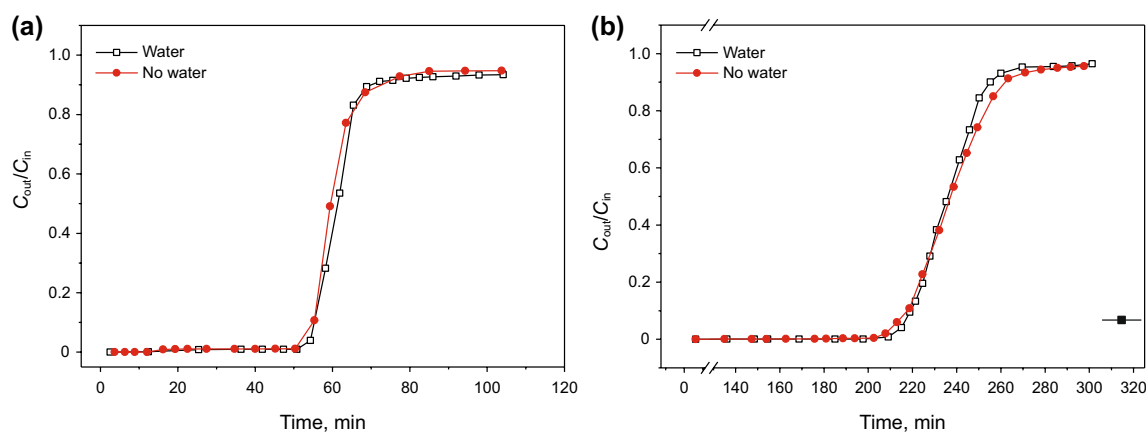
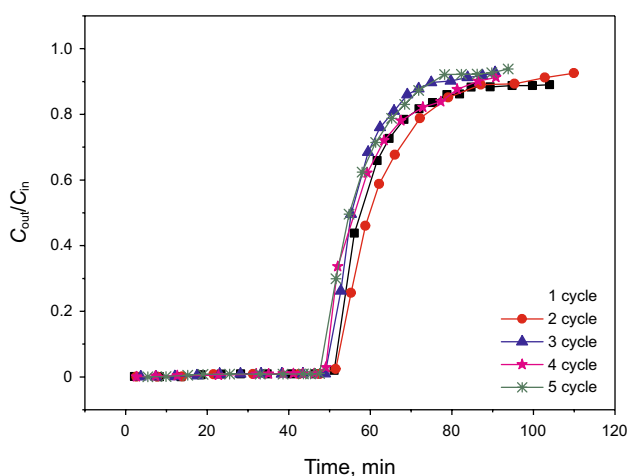**Fig. 8** Influence of the presence of water on the adsorption of L2 (**a**) and D4 (**b**)

Fig. 9 Adsorption breakthrough curves for L2 of the regenerated Ac@SG

4 Conclusions

Acetylated silica gel Ac@SG has been synthesized via treatment of microporous silica gel (SG) with acetic anhydride. Its meso-/microporous structure and hydrophobic surface exhibited better adsorption properties for siloxanes than simple SG. Dynamic adsorption experiments revealed that low temperatures and deep adsorbent beds of Ac@SG gave the best siloxane adsorption levels, with the presence of water having no significant effect on their performance. This Ac@SG adsorbent could be easily regenerated for reuse by heating at 110 °C, with its adsorption capacity for siloxanes remaining relatively constant when it was recycled in consecutive dynamic adsorption experiments.

References

Ahmed SA. Optimization and application of solid phase extraction of Cu(II) from aqueous solutions using new environmentally friendly modification of silica gel. J Environ Chem Eng. 2014;2:1713–21. https://doi.org/10.1016/j.jece.2014.06.011.

Ajhar M, Travesset M, Yüce S, et al. Siloxane removal from landfill and digester gas – A technology overview. Bioresour Technol. 2010;101:2913–23. https://doi.org/10.1016/j.biort ech.2009.12.018.

Allen MR, Braithwaite A, Hills CC. Trace organic compounds in landfill gas at seven U.K. Waste Disposal Sites. Environ Sci Technol. 1997;31:1054–61. https://doi.org/10.1021/es9605634.

An F, Gao B, Feng X. Adsorption of 2,4,6-trinitrotoluene on a novel adsorption material PEI/SiO$_2$. J Hazard Mater. 2009;166:757–61. https://doi.org/10.1016/j.jhazmat.2008.11.116.

Çimen A, Karakuş E, Bilgiç A. Chemical modification of silica gel with 4,4′-((1Z,8Z)-2,5,8-triazanona-1,8-diene-1,9-diyl) diphenol and applications to chromium Cr(VI) ions in industrial wastewaters. Desalin Water Treat. 2015;57:7219–31. https://doi. org/10.1080/19443994.2015.1014854.

Damja RI, Eaborn C. Preparation and reactions of some sterically hindered silanols, including [tris(trimethylsilyl)methyl] silanetriol. J Organomet Chem. 1985;290:267–75. https://doi. org/10.1016/0022-328x(85)87289-2.

De Arespacochaga N, Valderrama C, Mesa C, et al. Biogas deep clean-up based on adsorption technologies for solid oxide fuel cell applications. Chem Eng J. 2014;255:593–603. https://doi. org/10.1016/j.cej.2014.06.072.

Devia CR, Subrenat A. Absorption of a linear (L2) and a cyclic (D4) siloxane using different oils: application to biogas treatment. Environ Technol. 2013;34(23):3117–27. https://doi.org/10.1080/09593330.2013.804588.

Dewil R, Appels L, Baeyens J. Energy use of biogas hampered by the presence of siloxanes. Energy Convers Manage. 2006;47:1711–22. https://doi.org/10.1016/j.enconman.2005.10.016.

Eaborn C, Lickiss PD, Taylor AD. Reactions of the sterically hindered organosilicon diol (Me$_3$Si)$_2$C(SiMe$_2$OH)$_2$ and some of its derivatives. J Organomet Chem. 1988;340:283–92. https://doi.org/10.1016/0022-328x(88)80022-6.

Jafari T, Jiang T, Zhong W, et al. Modified mesoporous silica for efficient siloxane capture. Langmuir. 2016;32(10):2369–78. https://doi.org/10.1021/acs.langmuir.5b04357.

Jiang T, Zhong W, Jafari T, et al. Siloxane D4 adsorption by mesoporous aluminosilicates. Chem Eng J. 2016;289:356–64. https://doi.org/10.1016/j.cej.2015.12.094.

Kajolinna T, Aakko-Saksa P, Roine J, et al. Efficiency testing of three biogas siloxane removal systems in the presence of D5, D6, limonene and toluene. Fuel Process Technol. 2015;139:242–7. https://doi.org/10.1016/j.fuproc.2015.06.042.

Koner S, Pal A, Adak A. Adsorption of 2,4-D-herbicide from water environment on modified silica gel factory waste. Water Environ Res. 2013;85:2147–56. https://doi.org/10.2175/106143013X13736496909310.

Kougias PG, Angelidaki I. Biogas and its opportunities—A review. Front Env Sci Eng. 2018;12:1–13. https://doi.org/10.1007/s11783-018-1037-8.

Lee I, Rittmann BE. Using focused pulsed technology to remove siloxane from municipal sewage sludge. J Environ Eng. 2016;142:040150561–6. https://doi.org/10.1061/(ASCE)EE.1943-7870.0000975.

Machin WD, Golding PD. Adsorption of n-butane on silica gel. Langmuir. 1987;3:346–9. https://doi.org/10.1021/la00075a011.

Matsui T, Imamura S. Removal of siloxane from digestion gas of sewage sludge. Bioresour Technol. 2010;101:S29–32. https://doi.org/10.1016/j.biortech.2009.05.037.

Mobaraki N, Hemmateenejad B. Structural characterization of carbonyl compounds by IR spectroscopy and chemometrics data analysis. Chemometr Intell Lab. 2011;109:171–7. https://doi.org/10.1016/j.chemolab.2011.08.011.

Mota TRL, de Oliveira MAP, Nunes EHM, et al. Simple process for preparing mesoporous sol-gel silica adsorbents with high water adsorption capacities. Micropor Mesopor Mat. 2017;253:177–82. https://doi.org/10.1016/j.micromeso.2017.07.010.

Oshita K, Ishihara Y, Takaoka M, et al. Behaviour and adsorptive removal of siloxanes in sewage sludge biogas. Water Sci Technol. 2010;61:2003–12. https://doi.org/10.2166/wst.2010.101.

Pei ZF, Ponec V. On the intermediates of the acetic acid reactions on oxides: an IR study. Appl Surf Sci. 1996;103:171–82. https://doi.org/10.1016/0169-4332(96)00453-9.

Schweigkofler M, Niessner R. Removal of siloxanes in biogases. J Hazard Mater. 2001;B83:183–96. https://doi.org/10.1016/S0304-3894(00)00318-6.

Sigot L, Ducom G, Benadda B, et al. Adsorption of octamethyl-cyclotetrasiloxane on silica gel for biogas purification. Fuel. 2014;135:205–9. https://doi.org/10.1016/j.fuel.2014.06.058.

Sigot L, Ducom G, Germain P. Adsorption of octamethylcyclotetrasiloxane (D4) on silica gel(SG): retention mechanism. Micropor Mesopor Mat. 2015;213:118–24. https://doi.org/10.1016/j.micromeso.2015.04.016.

Sui DP, Chen HX, Li DW. Sol-gel-derived thiocyanato-functionalized silica gel sorbents for adsorption of Fe(III) ions from aqueous solution: kinetics, isotherms and thermodynamics. J Sol-Gel Sci Technol. 2016;80:504–13. https://doi.org/10.1007/s10971-016-4092-2.

Sui H, An P, Li X, et al. Removal and recovery of o-xylene by silica gel using vacuum swing adsorption. Chem Eng J. 2017a;316:232–42. https://doi.org/10.1016/j.cej.2017.01.061.

Sui H, Liu H, An P, et al. Application of silica gel in removing high concentrations toluene vapor by adsorption and desorption process. J Taiwan Inst Chem E. 2017b;74:218–24. https://doi.org/10.1016/j.jtice.2017.02.019.

Turkin AA, Dutka M, Vainchtein D, et al. Deposition of SiO$_2$ nanoparticles in heat exchanger during combustion of biogas. Appl Energy. 2014;113:1141–8. https://doi.org/10.1016/j.apenergy.2013.08.068.

Uruş S, Purtaş S, Ceyhan G, et al. Solid phase extraction of Pb(II), Cu(II), Cd(II) and Cr(III) with syringe technique using novel silica-supported bis(diazoimine) ligands. Chem Eng J. 2013;220:420–30. https://doi.org/10.1016/j.cej.2013.01.037.